Journal of Power Sources 191 (2009) 542–549

Contents lists available at ScienceDirect

Journal of Power Sources

journal homepage: www.elsevier.com/locate/jpowsour

Power management strategy for vehicular-applied hybrid fuel cell/battery power system

Xiangjun Li*, Liangfei Xu, Jianfeng Hua, Xinfan Lin, Jianqiu Li, Minggao Ouyang**

State Key Laboratory of Automotive Safety and Energy, Tsinghua University, Beijing 100084, China

ARTICLE INFO

Article history:
Received 5 December 2008
Received in revised form 20 January 2009
Accepted 28 January 2009
Available online 7 February 2009

Keywords:
Fuel cell hybrid vehicle
Fuel cell
Nickel-Metal Hydride battery
Fuzzy logic
Dynamic modeling

ABSTRACT

In this paper, a control strategy for a hybrid PEM (proton exchange membrane) fuel cell/BES (battery energy system) vehicular power system is presented. The strategy, based on fuzzy logic control, incorporates the slow dynamics of fuel cells and the state of charge (SOC) of the BES. Fuel cell output power was determined according to the driving load requirement and the SOC, using fuzzy dynamic decision-making and fuzzy self-organizing concepts. An analysis of the simulation results was conducted using Matlab/Simulink/Stateflow software in order to verify the effectiveness of the proposed control strategy. It was confirmed that the control scheme can be used to improve the operational efficiency of the hybrid power system.

1. Introduction

Environmental issues, energy crises, and concerns regarding peaking oil production have spurred research into and development of various types of hybrid electric vehicles. A fuel cell (FC)-powered hybrid vehicle is considered in this paper. Fuel cells offer high power density and low-to-zero emissions. Among the various FC types available, the proton exchange membrane (PEM) FC is the most promising for power systems to be used in automobile, residential, industrial, and other applications. The FC power converter system, for example, consists of a DC/DC converter to boost the stack voltage to a higher level, and a DC/AC inverter to drive the motor. Several variations of power converter architecture have been proposed in the literature [1–6], each entailing advantages and disadvantages.

In view of the fact that fuel cells alone might not be sufficient to satisfy the load demands in vehicular applications, in recent years, several control strategies for hybrid systems incorporating fuel cells and energy storage devices, such as super capacitors or/and batteries, have been presented. Meanwhile, intelligent control theory, for instance fuzzy logic and genetic algorithm, has been introduced to the control process. Because fuzzy control can readily incorporate human intelligence in complicated control practice based on human knowledge and experience. It has been demonstrated that a fuzzy controller is very effective to manage power flows in fuel cell powered vehicles hybridizing battery or/and ultracapacitors [6–10]. However, frequent load variations and unexpected driving conditions are inevitably uncertainties. Besides, aging stack and varying subsystems will cause the unsuitable output value obtained from pre-given fuzzy rule tables. In those foregoing reference papers, fuzzy control strategies have been focused on the pre-defined rule tables and an on-line self-organizing of fuzzy output value has not been considered. Hence, a fuzzy control strategy for instantaneous fuel cell power management including on-line self-organizing has been proposed. It is realized by modifying the fuzzy logic based output power of fuel cell. Moreover, to deal with the error in estimating the SOC, SOC diagnosis is introduced into the fuzzy control. That is, the judgment of charge upper limit and that of discharge lower limit are considered and they are introduced into fuzzy rule table indicated by very low (VL) and very high (VH), respectively.

The paper is organized as follows. Section 2 presents the structure of fuel cell powered vehicular power system. The model of the fuel cell system is described in Section 3 to properly represent the slow dynamics of fuel cell associated with the gas flows and the fuel processor operation. Then, the dynamic modeling of battery energy system is presented. Section 4 describes a fuzzy logic based power management strategy. Simulation results and validation analysis are discussed in Sections 5 and 6, respectively. Section 7 is the conclusions.

* Corresponding author. Tel.: +86 10 6278 5706; fax: +86 10 6278 5708.
** Co-corresponding author.
E-mail addresses: lixiangjun@tsinghua.edu.cn (X. Li), ouymg@tsinghua.edu.cn (M. Ouyang).

0378-7753/$ – see front matter © 2009 Elsevier B.V. All rights reserved.
doi:10.1016/j.jpowsour.2009.01.092

Nomenclature

Fuel cell system

B_{fc}, C_{fc}	constants to simulate the activation over voltage in FC system [A^{-1}] and [V]
E_{fcs}	Nernst instantaneous voltage [V]
E_{cell}^{ocv}	standard no load voltage [V]
F	Faraday's constant
K_{an}	anode valve constant
K_{H_2}	hydrogen valve molar constant
K_{H_2O}	water valve molar constant
K_r	modeling constant
M_{H_2}	molar mass of hydrogen
N_0	number of series fuel cells in stack
N_{fc_p}	number of fuel cell stacks in parallel
p_{H_2}	hydrogen partial pressure
p_{H_2O}	water partial pressure
p_{O_2}	oxygen partial pressure
q_{O_2}	input molar flow of hydrogen
$q_{H_2}^{in}$	hydrogen input flow
$q_{H_2}^{out}$	hydrogen output flow
$q_{H_2}^{r}$	hydrogen flow that reacts
I_{fc}	FC system current
R_{gas}	universal gas constant
R_{fc}^{int}	fuel cell internal resistance
T	absolute temperature
U	utilization rate
V_{an}	volume of anode
V_{fcs}	DC output voltage of FC system [V]
η_{act}	activation over voltage [V]
η_{ohmic}	ohmic over voltage [V]
τ_{H_2}	hydrogen time constant
τ_{O_2}	oxygen time constant
τ_{H_2O}	water time constant

Battery energy system

I_{bat}	battery current (A)
R_{bat}^{int}	internal resistance
R_{ch}	internal resistance of charge
R_{dis}	internal resistance of discharge
SOC	state of charge
SOC_{ini}	initial value of SOC
V_{ocv}	open circuit voltage of battery (V)
η	efficiency
η_{ch}	efficiency of charge
η_{dis}	efficiency of discharge

Power control strategy

P_{bat}	power of BES
P_{fc}	power of fuel cell system
P_{load}	demand of vehicular power system
P_{fc}^{min}	minimum power output of fuel cell system
P_{fc}^{max}	maximum power output of fuel cell system
P_{bat}^{min}	minimum power output of BES
P_{bat}^{max}	maximum power output of BES
P_{fc_net}	net power of fuel cell system
P_{stack}	fuel cell stack power output
P_{BOP}	auxiliary power for BOP
P_{fc_fuzzy}	fuel cell power fuzzy value
SOC_{ref}	reference value of SOC
SOC^{min}	minimum SOC
SOC^{max}	maximum SOC
SOC_{diag}	diagnoses status of SOC
V_{c_net}	mean voltage of each cell based on the net power for FC system
M	medium
S	small
VS	very small
L	low
VL	very low
H	high
VH	very high
N	normal
$-\Delta\bar{h}_f$	hydrogen's high heating value (286 kJ mol^{-1})
η_{fcs}	efficiency of fuel cell system
τ_{conv}	time constant of DC/DC converter

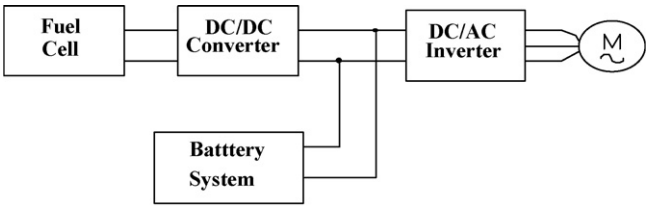

Fig. 1. Structure of vehicular power system.

2. Structure of FC-powered vehicular power system

The power system configuration is illustrated in Fig. 1. The FC system consists of two stacks in parallel. It is connected to a DC link via a DC/DC converter, the efficiency of which is assumed to be 90%. Directly connected to the DC link is a battery to supply the transient energy demand and peak loads required during acceleration and deceleration. Under transient conditions, and because the FC current dynamics were intentionally reduced, the battery supplies all other load variations. An electrical traction machine is fed by the DC bus via a DC/AC inverter, the efficiency of which is assumed to be 100%. That is only the power converter loss of the DC/DC converter is considered and that of the DC/AC inverter is ignored in this paper. The power output of DC/DC converter is assumed to be 90% of fuel cell output power. The vehicular power system as modeled by Matlab/Simulink/Stateflow software is illustrated in Fig. 2.

3. Performance and modeling of fuel cell and battery

3.1. Dynamic modeling of a PEM fuel cell system

The relationship between the molar flow of hydrogen through the valve and its partial pressure inside the channel can be expressed as [11]

$$\frac{q_{H_2}}{p_{H_2}} = \frac{K_{an}}{\sqrt{M_{H_2}}} = K_{H_2} \tag{1}$$

With regard to the hydrogen molar flow, there are three significant factors: hydrogen input flow, hydrogen output flow, and hydrogen flow during a reaction [11]. The relationship among these factors can be expressed as

$$\frac{d}{dt}p_{H_2} = \frac{R_{gas}T}{V_{an}}(q_{H_2}^{in} - q_{H_2}^{out} - q_{H_2}^{r}) \tag{2}$$

According to the basic electrochemical relationships between the hydrogen flow and the FC system current, the flow rate of

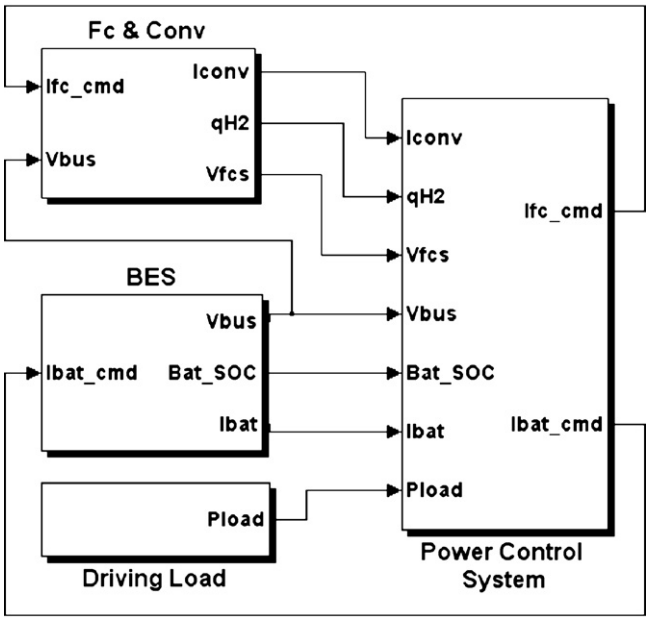

Fig. 2. Vehicular power system modeled by Matlab/Simulink/StateFlow.

reacted hydrogen is given by

$$q^r_{H_2} = \frac{N_0 I_{fc}}{2F} = 2K_r I_{fc} \tag{3}$$

Using Eqs. (1) and (3) and applying Laplace's transform, the hydrogen partial pressure can be obtained in the s domain, as in [11]

$$p_{H_2} = \frac{1/K_{H_2}}{1+\tau_{H_2} s}(q^{in}_{H_2} - 2K_r I_{fc}) \tag{4}$$

where

$$\tau_{H_2} = \frac{V_{an}}{K_{H_2} R_{gas} T} \tag{5}$$

Similarly, the water partial pressure and the oxygen partial pressure can be obtained. In the power system discussed in this paper, the two FC stacks, as already mentioned, are connected in parallel. The polarization curve for the PEM FC is obtained from the sum of Nernst's voltage, the activation over voltage and the ohmic over voltage. Assuming a constant temperature and oxygen concentration, the FC output voltage is presented as follows [1–2,5].

Table 1
PEM fuel cell system model parameters [1–2].

B_{fc}	0.04777 [A^{-1}]	τ_{O_2}	6.74 [s]
C_{fc}	0.0136 [V]	K_{O_2}	2.1×10^{-5} [kmol s^{-1} atm^{-1}]
E_0	0.95 [V]	K_{H_2O}	7.716×10^{-6} [kmol s^{-1} atm^{-1}]
N_0	350	τ_{H_2}	3.37
N_{fc_p}	2	K_{H_2}	4.22×10^{-3} [kmol s^{-1} atm^{-1}]
R_{gas}	8314.47 [J $kmol^{-1}$ K^{-1}]	U	0.8
K_r	9.0688×10^{-7} [kmol s^{-1} A^{-1}]	$r_{H.O}$	1.168
R^{int}_{fc}	0.177 [Ω]	T	343 [K]

$$V_{fcs} = E_{fcs} + \eta_{act} + \eta_{ohmic} \tag{6}$$

where

$$\eta_{act} = -B_{fc} \ln(C_{fc} I_{fc}) \tag{7}$$

$$\eta_{ohmic} = -R^{int}_{fc} I_{fc} \tag{8}$$

The Nerst's instantaneous voltage may be expressed as [5]

$$E_{fcs} = N_0 \left[E^{ocv}_{cell} + \frac{R_{gas} T}{2F} \log \left[\frac{p_{H_2} \sqrt{P_{O_2}}}{p_{H_2O}} \right] \right] \tag{9}$$

The FC system consumes hydrogen according to the power demand. The hydrogen required for stack operation is obtained from a high-pressure hydrogen tank. The Matlab/Simulink-based FC system model and the parameters of the PEM FC system model are shown in Fig. 3 and listed in Table 1, respectively. The PEMFC system model presented is simple and it does not account for some of the most important challenges present on PEMFC operation such as water and heat management. PEMFC stack resistance depends strongly on the level of hydration of the stack.

3.2. Dynamic modeling of battery energy system

A Nickel-Metal Hydride battery (Ni-MH battery) was modeled in reference to the R_{int} model presented in Ref. [12]. The Ni-MH battery energy system consists of four 80 Ah sub batteries in series. In general we know that I_{bat} and V_{bat} can be expressed as Eqs. (10) and (11), respectively, when the battery power consumption is P

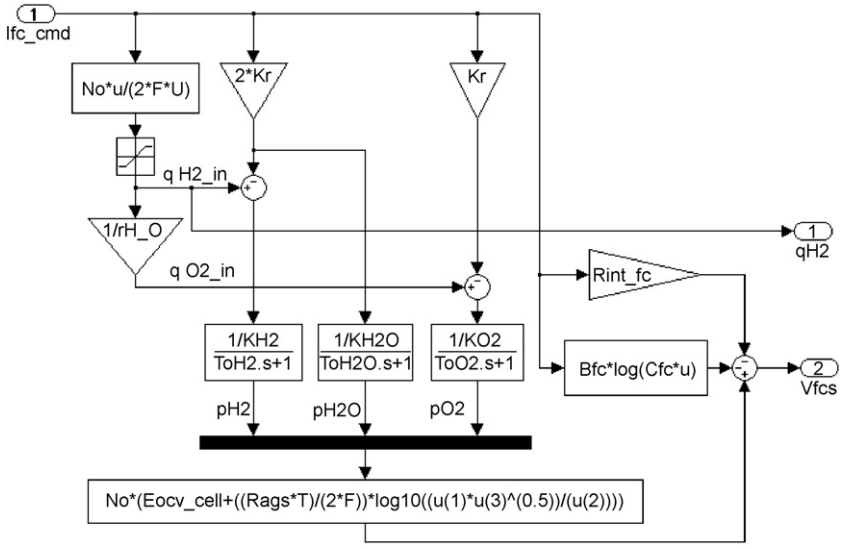

Fig. 3. Dynamic model of fuel cell system.

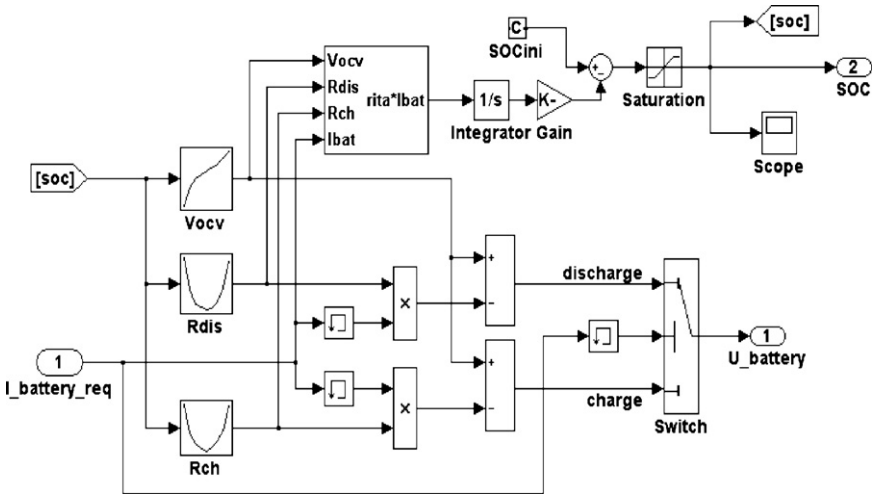

Fig. 4. Dynamic model of battery energy system.

W. A simple dynamic model of battery energy system is shown in Fig. 4. As shown in Fig. 4 and Eqs. (12) and (13), V_{ocv} and R_{bat}^{int} are determined by using look-up tables based on experimental data presented in Fig. 5. In this paper, SOC is calculated by Eqs. (14) and (15). As shown in Eq. (15), the η in Eq. (14) is calculated depend on the battery charge/discharge status.

$$I_{bat} = \frac{V_{ocv} - \sqrt{V_{ocv}^2 - 4R_{bat}^{\text{int}}P}}{2R_{bat}^{\text{int}}} \tag{10}$$

$$V_{bat} = V_{ocv} - R_{bat}^{\text{int}} I_{bat} \tag{11}$$

where

$$V_{ocv} = f_1(SOC) \tag{12}$$

$$R_{bat}^{\text{int}} = \begin{cases} R_{ch} = f_2(SOC) & \text{charging} \\ R_{dis} = f_3(SOC) & \text{discharging} \end{cases} \tag{13}$$

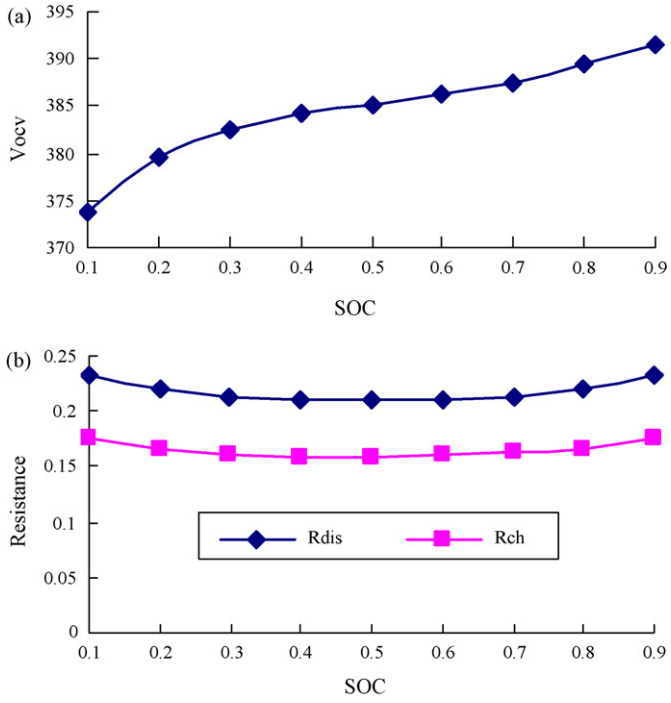

Fig. 5. Characteristic of Ni-MH battery energy system.

$$SOC = SOC_{ini} - \int \frac{\eta I_{bat}}{Q}\,dt \tag{14}$$

$$\eta = \begin{cases} \eta_{ch} = \dfrac{V_{ocv}}{V_{ocv} - I_{bat}R_{ch}} & \text{charging} \\ \eta_{dis} = \dfrac{V_{ocv} - I_{bat}R_{dis}}{V_{ocv}} & \text{discharging} \end{cases} \tag{15}$$

4. Fuzzy logic based power management strategy

FC system efficiency can be defined as the ratio between electricity produced and hydrogen consumed, and is expressed as follows [13].

$$\eta_{FCS} = \frac{V_{c\_net}}{-\Delta\bar{h}_f/2F} = \frac{V_{c\_net}}{1.482} \tag{16}$$

The mean voltage V_{c_net} can be calculated as

$$V_{c\_net} = \frac{P_{fc\_net}}{I_{fc}} = \frac{P_{Stack} - P_{BOP}}{I_{fc}} \tag{17}$$

In this paper, P_{BOP} is simply assumed to scale linearly with fuel cell output current to present the typical efficiency characteristic of fuel cell system. As a result, the net FC system efficiency is shown in Fig. 6. Therefore, the purpose of the power management strategy is to control the fuel cell power output at optimal operating conditions. The *V–I* characteristic of fuel cell system is shown in Fig. 7.

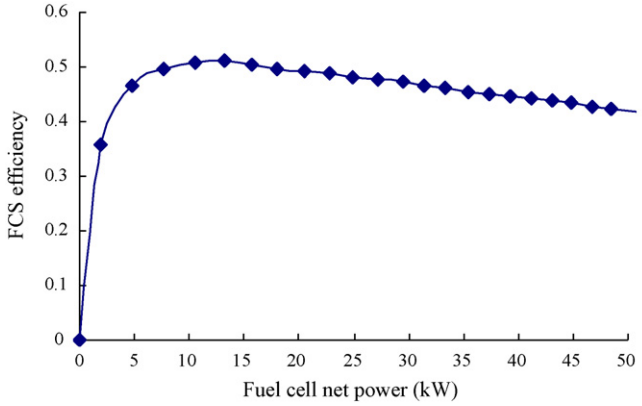

Fig. 6. Net fuel cell system efficiency.

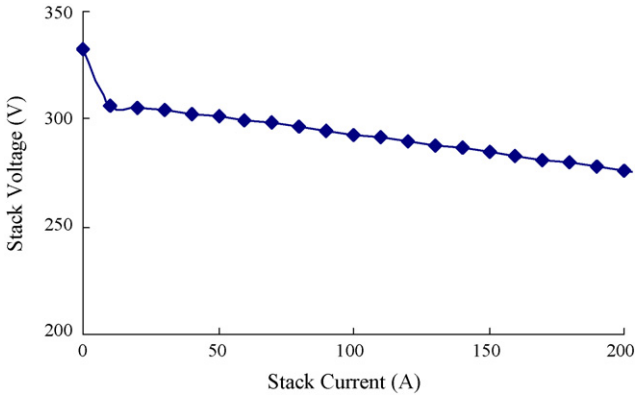

Fig. 7. *V–I* characteristic of fuel cell system.

In order to operate the FC system efficiently, low efficient operating conditions should be avoided, as presented in Fig. 6. Therefore, under normal state of SOC, the $P_{fc}^{\min}$ and $P_{fc}^{\max}$ for each stack were set to 4 kW and 40 kW, respectively. However, when the SOC becomes abnormal, $P_{fc}^{\min}$ will be set to 0 kW. The method of diagnosing abnormal SOC is described at the end of this section.

This paper makes use of a PEM fuel cell as the main power source and accordingly BES is the complementary source. The power balance of system can be expressed as

$$P_{fc} + P_{bat} = P_{load} + P_{loss} \tag{18}$$

subject to

$$P_{fc}^{\min} \le P_{fc} \le P_{fc}^{\max} \tag{19}$$

$$P_{bat}^{\min} \le P_{bat} \le P_{bat}^{\max} \tag{20}$$

where, P_{loss} is only calculated by the power converter loss of the DC/DC converter in this paper.

The fuel cell power output P_{fc} is calculated based on the SOC of battery and power demand P_{load} as follows.

$$P_{fc} = P_{fc\_fuzzy}\left[1 + \frac{SOC_{ref} - SOC}{(SOC^{\max} - SOC^{\min})/2}\right] \tag{21}$$

where

$$P_{fc\_fuzzy} = f(SOC, P_{load}, SOC_{diag}) \tag{22}$$

$$SOC_{ref} = \begin{cases} 0.6 & if\ SOC < 0.5 \\ 0.6 & if\ SOC > 0.7 \\ SOC & otherwise \end{cases} \tag{23}$$

As shown in Eqs. (21), (22) and (23), fuzzy logic is utilized in the power control strategy and the design variables really being controlled are mainly P_{fc_fuzzy} and SOC_{ref} to achieve the above mentioned control goal. This paper proposes a Mamdani type's fuzzy logic controller (FLC), in which three inputs are SOC, power demand, and a diagnoses status of SOC (SOC_{diag}) and one output is P_{fc_fuzzy} as shown in Eq. (22). The fuzzy membership functions of the SOC, P_{load}, SOC_{diag} and P_{fc_fuzzy}, are shown in Fig. 8. A fuzzy rule table for P_{fc_fuzzy} is Table 2. The frame of the power control procedure is shown in Fig. 9. It can be seen that to operate fuel cell system at optimal operating conditions, state machine is used in the P_{fc} identification block. That is, the three states can be explained in the following: (1) normal model: if P_{fc} determined by Eq. (21) is within allowable values, P_{fc} is not changed; (2) lower limit model: if P_{fc} determined by Eq. (21) is less than $P_{fc}^{\min}$, set $P_{fc} = P_{fc}^{\min}$, as a result, avoiding the fuel cell system operated at low efficient region; (3) upper limit model: if P_{fc} determined by Eq. (21) is large than $P_{fc}^{\max}$, set $P_{fc} = P_{fc}^{\max}$, thus, also avoiding the fuel cell system operated at low efficient region.

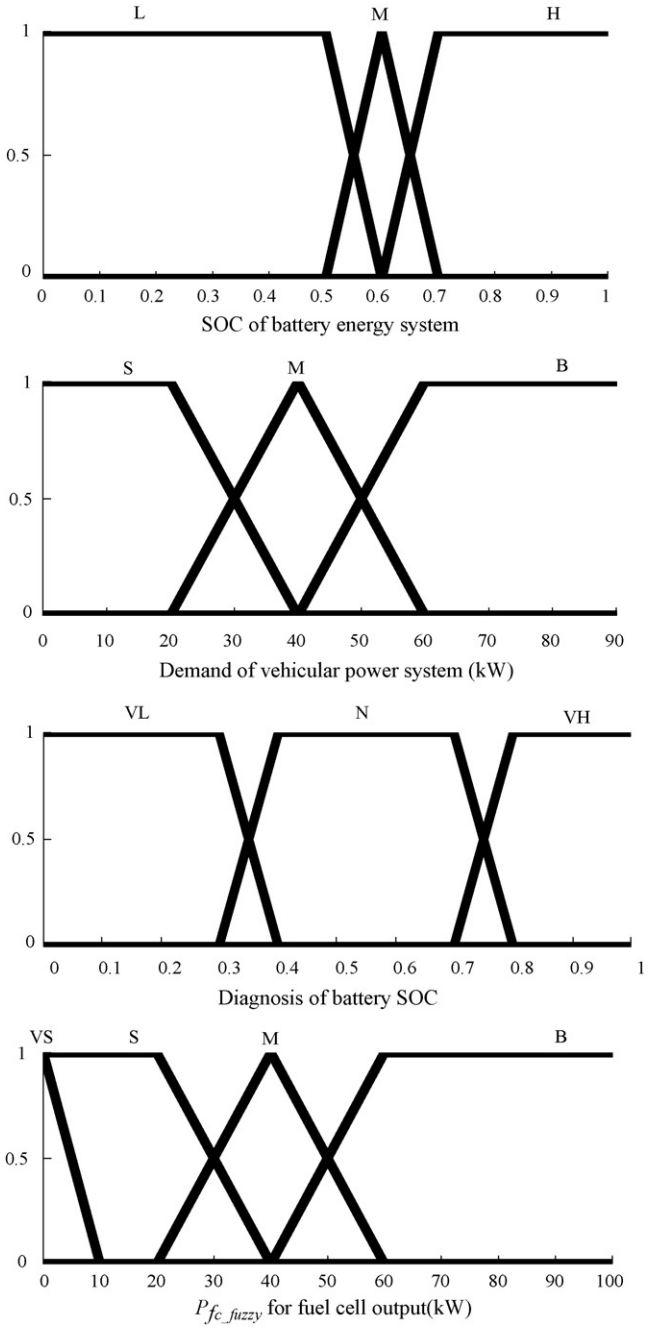

Fig. 8. Fuzzy membership function.

Table 2
Fuzzy rule table for P_{fc_fuzzy}.

No.	Logic of judgment rules
1–3	If SOC is L & P_{load} is S & SOC_{diag} is N/VL/VH then P_{fc_fuzzy} is S/M/VS
4–6	If SOC is L & P_{load} is M & SOC_{diag} is N/VL/VH then P_{fc_fuzzy} is M/M/VS
7–9	If SOC is L & P_{load} is B & SOC_{diag} is N/VL/VH then P_{fc_fuzzy} is B/M/VS
10–12	If SOC is M & P_{load} is S & SOC_{diag} is N/VL/VH then P_{fc_fuzzy} is S/M/VS
13–15	If SOC is M & P_{load} is M & SOC_{diag} is N/VL/VH then P_{fc_fuzzy} is M/M/VS
16–18	If SOC is M & P_{load} is B & SOC_{diag} is N/VL/VH then P_{fc_fuzzy} is B/M/VS
19–21	If SOC is H & P_{load} is S & SOC_{diag} is N/VL/VH then P_{fc_fuzzy} is S/M/VS
22–24	If SOC is H & P_{load} is M & SOC_{diag} is N/VL/VH then P_{fc_fuzzy} is S/M/VS
25–27	If SOC is H & P_{load} is B & SOC_{diag} is N/VL/VH then P_{fc_fuzzy} is M/M/VS

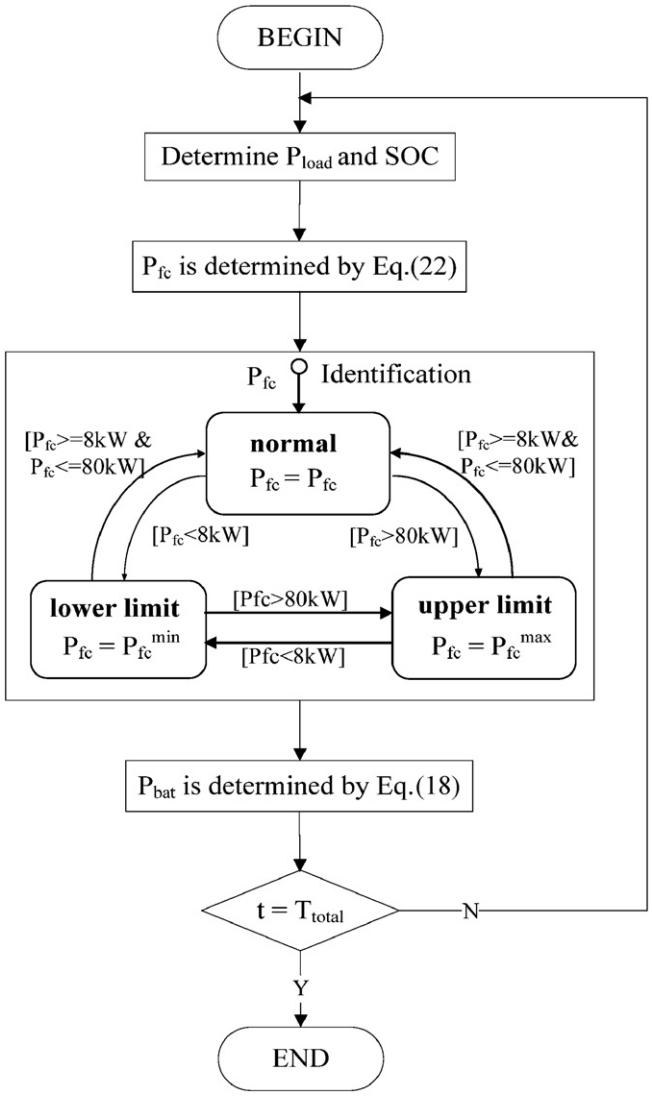

Fig. 9. Frame of the power control procedure.

The foregoing functions are realized by Stateflow software in this paper.

The SOC is not always an easy value to evaluate. We deal with the error in estimating the SOC by using diagnosis table as shown in Table 3. As shown in this table, two critical states of SOC, very low and very high, are considered when SOC estimating errors are cumulated. Moreover, the states are proposed into FLC to diagnose the battery SOC as shown in Fig. 8.

Sometimes, the fuzzy control rule made in advance cannot effectively satisfy fuel cell operation requirement because of the stack aging and real-time driving cycle, etc. Therefore, this paper suggests a self-organizing method to revise the fuel cell output power based on fuzzy rule to control the SOC between 0.5 and 0.7. The procedure of deciding SOC_{ref} is shown in Fig. 10. It can be seen that to ensure

Table 3
Diagnosis table to estimate the critical status of battery SOC.

	SOC is very high for charge model	SOC is very low for discharge model
1	$0 \le \lvert I_{bat}\rvert \le 1C$ and $V_{module} \ge 14.3V$	$0 \le I_{bat} \le 1C$ and $V_{module} \le 12.3V$
2	$1C < \lvert I_{bat}\rvert \le 1.5C$ and $V_{module} \ge 14.7V$	$1C < I_{bat} \le 2C$ and $V_{module} \le 11.8V$
3	$1.5C < \lvert I_{bat}\rvert \le 2C$ and $V_{module} \ge 15.1V$	$2C < I_{bat} \le 3C$ and $V_{module} \le 11.5V$
4	$\lvert I_{bat}\rvert > 2C$ and $V_{module} \ge 15.5V$	$I_{bat} > 3C$ and $V_{module} \le 11V$

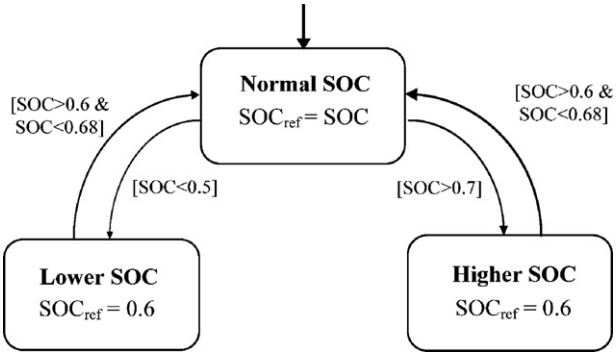

Fig. 10. Logic of SOC_{ref} decision.

SOC at expected status, a state machine is also used to realize this goal by modifying SOC_{ref}.

As previously discussed, the power output of fuel cell is controlled to satisfy a slow dynamic variation which is achieved by multiplying a filter K_{filter} in the Eq. (21). The K_{filter} is used to control the DC/DC output current and determined as

$$K_{filter} = \frac{1}{1 + \tau_{conv} s} \tag{24}$$

where τ_{conv} is a time constant for DC/DC converter and it is set to 2 in this paper.

5. Simulation result and analysis

To evaluate the proposed control method, a cyclical driving simulation was conducted using the MATLAB/Simulink/Stateflow software. The SOC target value can be changed for different applications, and in the simulation, the range of between 0.5 and 0.7 was selected. A cycle driving load mode was assumed as shown in Fig. 11. The maximum load power was about 60 kW. The SOC^{max} and SOC^{min} were assumed to be 0.8 and 0.2, respectively. The simulation results are presented as follows.

Fig. 12 shows the power profile for the initial SOC of 0.7. As shown in Fig. 12, the battery discharges rapidly to react to the fast load changes and to supply the supplementary power, because the output power change of the FC stack is intentionally restricted to a slow dynamic response in order to extend the lifetime of the FC system. Meanwhile, the FC power is used dynamically to charge the battery, thus maintaining the SOC target value when the load power is lower or zero. Fig. 13 shows the distribution percentage for the fuel cell output power. It is illustrated that the fuel cell system is operated at high efficiency scopes.

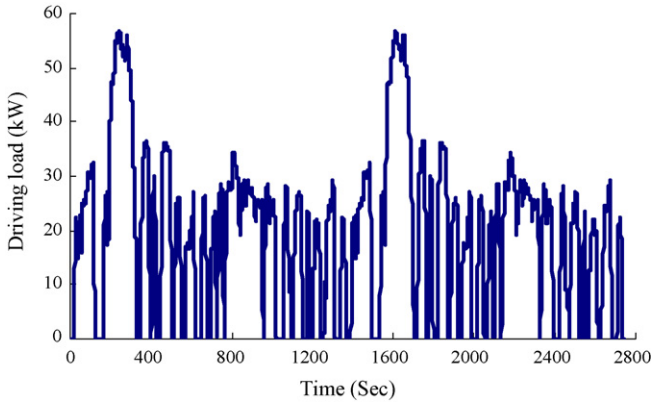

Fig. 11. Load profile for single-cycle simulation.

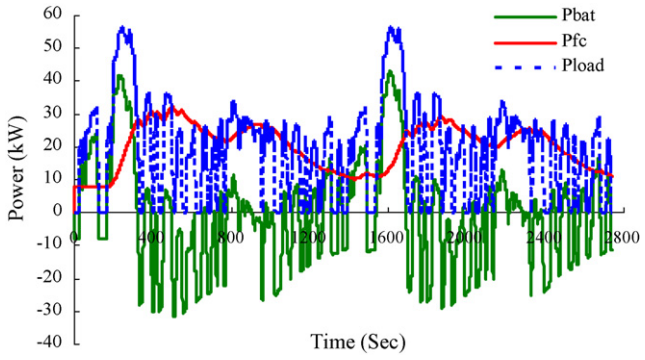

Fig. 12. Power profile for initial SOC of 0.7.

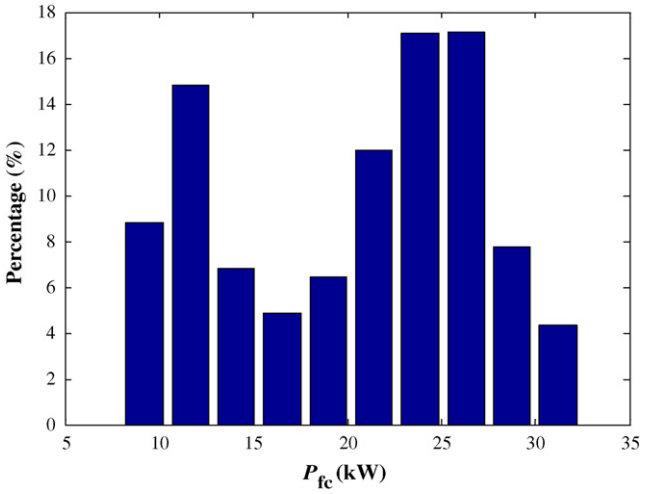

Fig. 13. Distribution percentage of fuel cell output power.

Fig. 14 shows the power profile for the initial SOC of 0.7. In Fig. 14, it is evident that, using the proposed control methodology, the SOC of the battery energy system can be maintained around the target range. Meanwhile, the battery voltage is changed as shown in Fig. 15.

Fig. 16 shows the change of SOC considering different initial SOC of battery energy system. It is obtained from a case of setting a target SOC of 0.7 during the cycle's driving simulation. From this figure, it is apparent that the SOC of the battery can be effectively maintained around the target value of 0.7 by using the proposed fuzzy modification concept to flexibly adjust the fuzzy logic based FC power output.

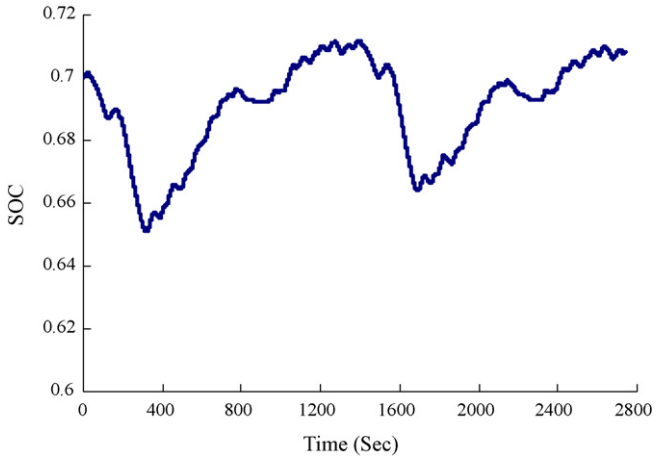

Fig. 14. SOC profile for initial SOC of 0.7.

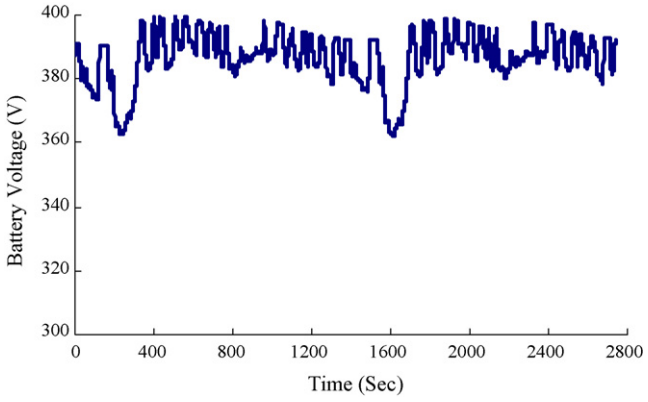

Fig. 15. Battery voltage profile for initial SOC of 0.7.

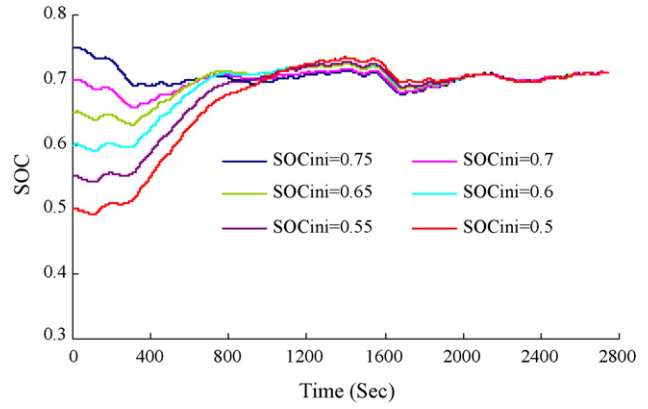

Fig. 16. Change of SOC according to different initial SOC.

6. Validation and analysis

To evaluate the performance of the proposed power control strategy, some road driving tests were conducted using fuel cell hybrid vehicle (FCHV) shown in Fig. 17. The FCHV began operating as part of a 1-year-long Olympic demonstration in Beijing [14]. The specifications of the FCHV are shown in Table 4. Fig. 18

Fig. 17. Fuel cell hybrid vehicle.

Table 4
Specifications of FCHV in Beijing.

1	Fuel cell system	
	Type	PEM
	Output voltage	360–520 V
	Cooling mode	Water
2	Hydrogen	
	Type	Pure
	Rated hydrogen vessel pressure	20 Mpa
3	DC/DC converter	
	Type	Buck
	Input voltage	360–520 V
	Output voltage	300–420 V
	Cooling mode	Water
4	Battery system	
	Type	Nickel-Metal Hydride
	Nominal voltage	336 V
	Capacity	80 Ah
	No. of modules	28
5	Motor	
	Type	Induction
	Rated power	100 kW
	Maximum output power	185 kW
	Maximum output torque	1100 Nm
	Maximum rotate speed	6000 rpm
	Cooling mode	Water

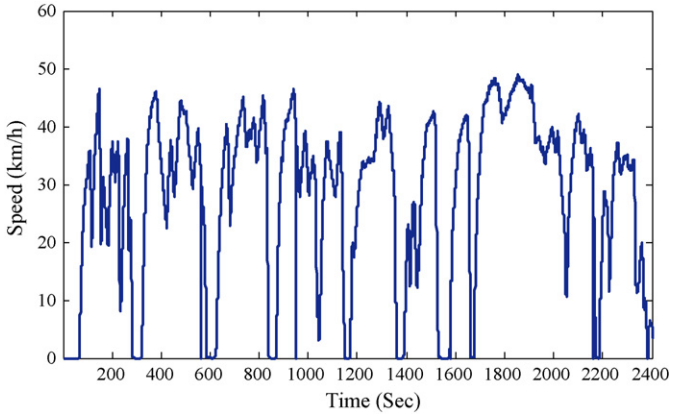

Fig. 18. Vehicle speed profile during road test driving period.

shows vehicle speed profile during 2400 s road test driving period. Figs. 19 and 20 show the test results for the FCHV, where the power train was controlled by the proposed power management strategy using fuzzy logic. From Figs. 19 and 20, it can be seen that the SOC

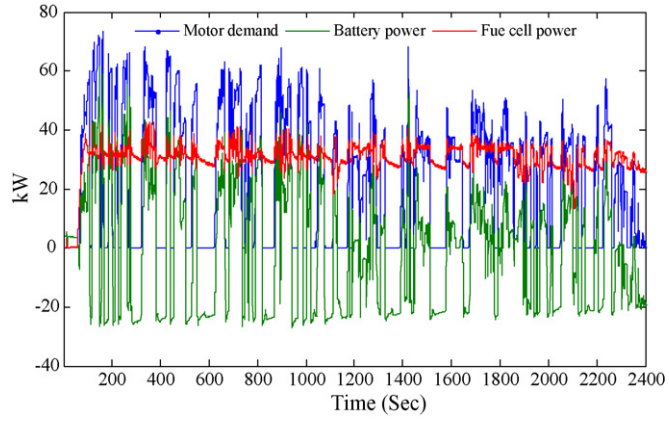

Fig. 19. Test result of power profile for FCHV.

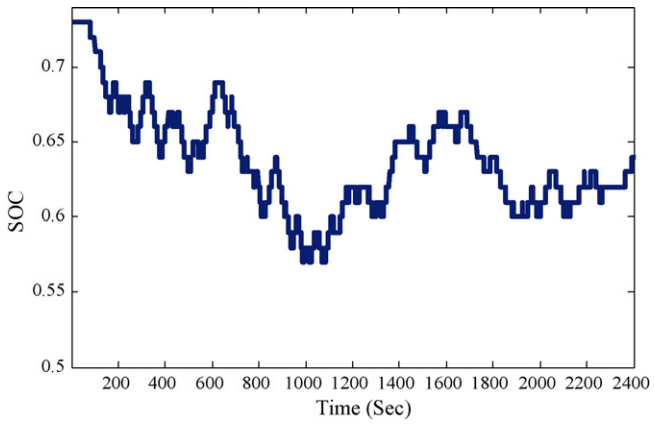

Fig. 20. Test result of SOC profile for FCHV.

of battery can be maintained around the target conditions through real-time power flow control.

7. Conclusions

In this paper, a fuzzy logic based power management strategy that secures the power balance and maintains the SOC in a hybrid FC vehicular power system is proposed. Simulation results and road driving tests demonstrate that the proposed method can control the FC system within a specified high-efficiency region and manage the system power flows to maintain the SOC of the battery around the target conditions. The optimal power control including hydrogen utilization will be discussed in the near future with a regenerative braking control of fuel cell hybrid vehicle.

Acknowledgements

This work is supported by the National Energy-efficient and New Energy Vehicle Program-Research and Development of Fuel Cell City Bus Power System Technology Platform, which belongs to the eleventh five year “863” program-the hi-tech research and development program of China.

References

[1] M. Uzunoglu, M.S. Alam, IEEE Transactions on Energy Conversion 23 (1) (2008) 263–272.
[2] M. Uzunoglu, M.S. Alam, Energy Conversion and Management 48 (2007) 1544–1553.
[3] Joeri Van Mierlo, Yonghua Cheng, Jean-Marc Timmermans, Peter Van den Bossche, Comparison of Fuel Cell Hybrid Propulsion Topologies with Super-Capacitor, EPE-PEMC, 2006, pp. 501–505.
[4] A. Abedini, A. S Nasiri, Modeling and Analysis of Hybrid Fuel Cell Systems for Vehicular Applications, IEEE Vehicle Power and Propulsion Conference, 2006, pp. 1–6.
[5] M.Y. El-Sharkh, A. Rahman, M.S. Alam, P.C. Byrne, A.A. Sakla, T. Thomas, Journal of Power Sources 138 (1–2) (2004) 199–204.
[6] Dawei Gao, Zhenhua Jin, Qingchun Lu, Journal of Power Sources 185 (2008) 311–317.
[7] Amir Poursamad, Morteza Montazeri, Control Engineering Practice 16 (2008) 861–873.
[8] Minjin Kim, Young-Jun Sohn, Won-Yong Lee, Chang-Soo Kim, Journal of Power Sources 178 (2008) 706–710.
[9] Kwi-Seong Jeong, Won-Yong Lee, Chang-Soo Kim, Journal of Power Sources 145 (2005) 319–326.
[10] Naim A. Kheir, Mutasim A. Salman, Niels J. Schouten, Mathematics and Computers in Simulation 66 (2004) 155–172.
[11] J. Padulles, G.W. Ault, J.R. McDonald, Journal of Power Sources 86 (2000) 495–500.
[12] National Renewable Energy Laboratory, ADVISOR Documentation, April 30, 2002.
[13] J. Larminie, A. Dicks, Fuel Cell Systems Explained, second ed., Wiley, 2003.
[14] Jianfeng Hua, Xinfan Lin, Liangfei Xu, Jianqiu Li, Minggao Ouyang, Journal of Power Sources 186 (2009) 478–484.